

Lasers in Manufacturing Conference 2021

## Acoustic emissions of laser metal deposited NiTi structures

Julian Ulrich Weber<sup>a,\*</sup>, Alexander Bauch<sup>a</sup>, Johannes Jahnke<sup>a</sup>, Claus Emmelmann<sup>b</sup>

<sup>a</sup>Fraunhofer IAPT, Am Schleusengraben 14, Hamburg and 21029, Germany

<sup>b</sup>Institute of Laser and System Technologies iLAS, Denickestr. 17, Hamburg and 21073, Germany

---

### Abstract

Laser Metal Deposition (LMD) is an additive manufacturing process that enables the metal part production of complex near net-shape parts. Precise material deposition increases material efficiency and prevents the excessive use of costly materials. In a fully automated manufacturing process with minimized scrap production, these benefits are enabled by material specific process monitoring and parameter development.

Acoustic emissions were monitored for the LMD process of the costly shape memory alloy. Acoustic emission monitoring values were defined and evaluated regarding of NiTi structural defect formation. For the evaluation of defect formation, the degree of delamination for each specimen has been identified. Concurrent measurement of the oxygen content in the process chamber was carried out to correlate defects to the process atmosphere.

Distinct defect frequencies were detected for NiTi structures indicating delamination and cracks. The acquired data was used to design an LMD process control concept based on acoustic emission monitoring.

Keywords: Laser Metal Deposition; Acoustic Emissions; Nickel-Titanium; Nitinol; Defect monitoring

---

### 1. Introduction

Laser Metal Deposition (LMD) is an additive manufacturing process used either to produce metallic coatings on existing part components or to build up near net-shape three-dimensional structures on given substrate materials. A laser beam is used to create a surface melt pool of the substrate material, while at the same time metallic powder material is fed to the melt pool. After solidification of the melt pool, metallic structures are

---

\* Corresponding author.

E-mail address: julian.ulrich.weber@iapt.fraunhofer.de.

formed layer-wise. This process offers the opportunity to manufacture complex structures with a high material efficiency and high deposition rates. Therefore, LMD presents a favorable manufacturing technique for materials that are costly to process, such as Nickel-Titanium (NiTi) shape memory alloys (SMAs).

NiTi structures can be used as smart materials with integrated actuator functions by applying temperature changes that result in geometrical changes according to its shape memory effect (Kauffman and Mayo, 1997). Krishna et al., 2007 and Halani et al., 2012 evaluated the feasibility to manufacture NiTi structures by LMD, while Scheitler et al., 2017 investigated optimized LMD processing strategies, including substrate pre-heating. However, producing NiTi on dissimilar substrate materials such as Ti sheet metals, defect signatures such as cracks, pores or delamination might occur (Scheitler et al., 2017).

The influence of oxygen ( $O_2$ ) concentrations on Ti-based alloys is well researched (Engblom Eyvind, 2018), the influence different of  $O_2$  concentrations while LMD processing of NiTi structures has not been focused in research yet.

In order to enable a high degree in automation, extensive process parameter development, cost-intensive pre-heating or monitoring techniques are required. Tang et al., 2020 reviewed In-Situ monitoring technologies for Directed Energy Deposition (DED) processes, focusing on the manufacture of metal structures. It is shown, that Acoustic Emission (AE) monitoring and its corresponding data analysis can be used to analyze metallurgical defects, such as crack generation and expansion (Wang et al., 2008). Gaia and Liou, 2016 and Taheri et al., 2019 evaluated data processing techniques like K-means clustering to indicated defect formation. However, no investigations of acoustic monitoring techniques have been conducted for the LMD process of NiTi structures.

This paper aims gain knowledge regarding acoustic emission monitoring values for LMD of NiTi. Further, this paper aims to gain knowledge about defect formation for LMD of NiTi structures, dependent on various  $O_2$  level concentrations.

## 2. Experimental setup and materials

### 2.1. LMD setup

The experimental setup contained a Nd:YAG laser mounted on a 3-axis computer controlled kinematic system, with a wave length of 1070 nm and a maximum laser power of 300 W. The air-cooled laser can be used in continues wave or pulsed mode, with a pulse duration of 0.5-50 ms. Due to the lasers beam parameter product of 10 mm x mrad and a movable 200 mm focus lens the focus spot diameter could be adjusted between 0.48 and 3.52 mm.

The LMD process was shielded by argon gas (Ar), which is also used for the generation of an inert gas atmosphere within a processing chamber and as carrier gas for the powder feeding system. The powder mass flow was controlled by a disk-conveying powder feeding system. LMD experiments were carried out using pre-alloyed NiTi powder material in range of 45 to 100  $\mu\text{m}$ . The nickel content amounts to 50.8 at. %. The titanium content amounts to 49.2 at. %. The morphology of the powder particles is considered spherical.

### 2.2. Monitoring setup

For the recording of acoustic emissions, a directional microphone (*Sennheiser MKE 600*) was used. The frequency of the capacitor microphone ranges from 40 Hz to 20 kHz. The geometrical monitoring performance is characterized as super cardioid. The microphone was mounted on a tripod with an included vibration damping function. Further physical contact of the setup to the process cell was kept to a minimum to reduce structure borne noise.

The raw sensor output was transformed into a digital signal by an audio interface (*Behringer U-Phoria UMC202HD*) with a sampling rate of 192 kHz. Channel gains were applied by the audio interface and kept constant throughout the whole manufacturing process. After monitoring, the acquired data was exported via USB connection to a computer with a 24-bit resolution. Data processing and storing was performed manually using the computational software *MATLAB* and the audio editor *Audacity*.

O<sub>2</sub> concentration monitoring was performed using an amperometric O<sub>2</sub> sensor, based on an electro-chemical zirconium dioxide gas-pumping cell. The sensor is able to detect O<sub>2</sub> concentrations between 10 and 1000 ppm. Measurement values were sent via RS232 interface to a local computing unit, where data was captured and evaluated using *MATLAB*. The experimental setup is schematically illustrated in Fig. 1.

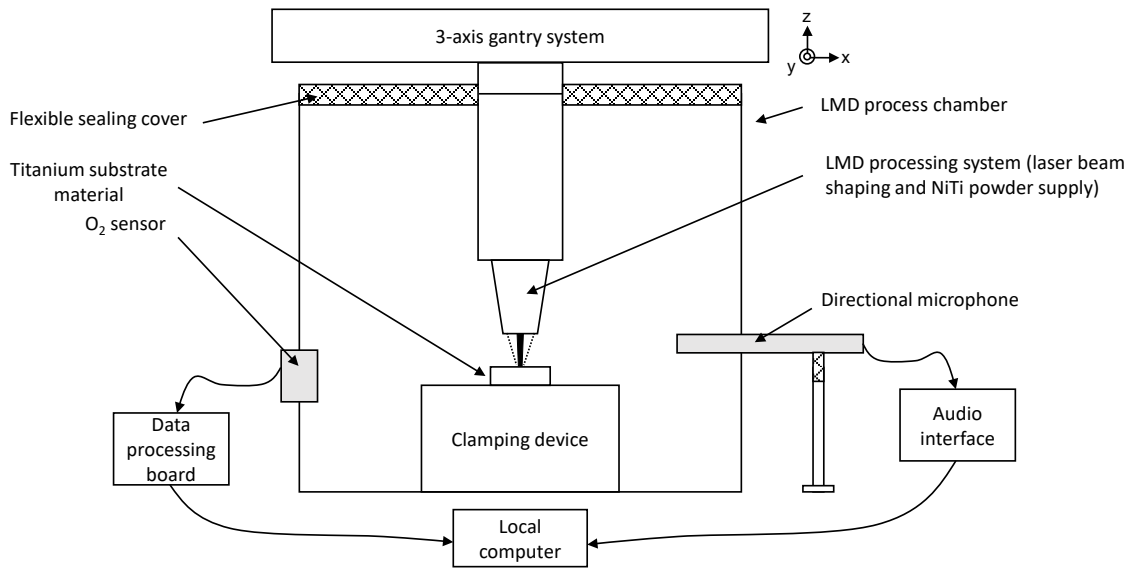


Fig. 1. Experimental setup of the LMD and monitoring process

### 2.3. Experimental plan

Identical process parameter sets were performed at 6 different O<sub>2</sub> concentration levels. The level of O<sub>2</sub> concentration within the process chamber was controlled by setting the shielding gas input for the process chamber. Identical build-up process strategies were selected and performed, so that defect deformation (e.g. delamination) will occur. One different process parameter set was performed, to trigger further defect deformations within the NiTi structure. Acoustic emissions and residual O<sub>2</sub> concentrations were monitored during the manufacture of NiTi structures on titanium substrate. All process parameters are summarized in Table 1.

Table 1. LMD process parameters for the deposition of NiTi structures

Process parameters	Unit	1	2	3	4	5	6	7
Average O <sub>2</sub> concentration	[ppm]	77,32	127,11	151,65	190,84	256,87	290,74	189,29
Laser power	[W]	150	150	150	150	150	150	150

Focal spot diameter	[mm]	0,48	0,48	0,48	0,48	0,48	0,48	0,48 - 3,52
Welding speed	[mm/s]	11,5	11,5	11,5	11,5	11,5	11,5	11,5
Material feed rate	[g/min]	2,15	2,15	2,15	2,15	2,15	2,15	2,15
Shielding gas rate	[l/min]	5	5	5	5	5	5	5

All NiTi samples were manufactured onto titanium sheet material. The structures were designed as a rectangular shape measuring 30 mm in length, 5 mm in width and 0,5 mm in height, using hatch distance of 550  $\mu\text{m}$  and a track height of 165  $\mu\text{m}$ . Specimen analysis included the investigation of geometrical outer dimensions and optical appearance evaluation. For this purpose, high quality photographic shoots were performed of each sample using a DSLR camera with a macro objective lens.

### 3. Results and discussion

#### 3.1. Acoustic emissions of NiTi LMD process

While processing the NiTi structures, distinct defect noises were clearly audible. Fig. 2 shows on the upper left side the raw audio signal in normalized amplitude over time of the manufacturing process of specimen 1. The corresponding frequency spectrogram is used to identify distinct defect frequencies and shows all occurring frequencies with each frequency amplitude in dB on the lower left side. To allocate distinct frequencies to its sound events, such as environmental (machine axes, surrounding machinery) or process frequencies, and focus on process relevant frequencies, a frequency spectrogram was performed over time.

The analysis over the full monitoring period shows, that the highest amplitude of frequencies are specified by low frequencies between 0 and 2000 Hz. Separate analysis of this frequency band shows, that mainly environmental noises are covered by frequencies up to 2000 Hz. Thus, further recordings and audio investigations cut out all frequencies below 2000 Hz.

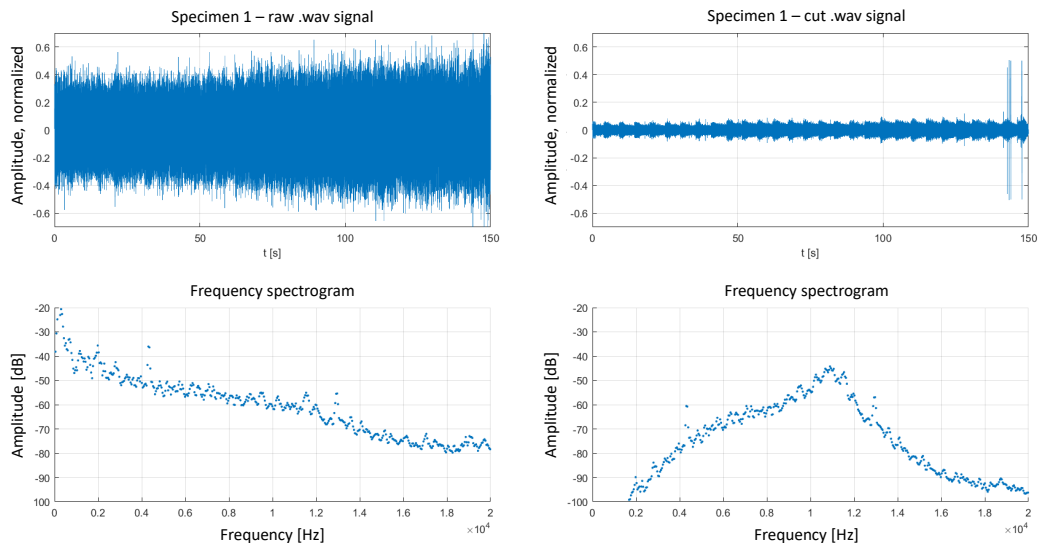


Fig. 2. Acquired acoustic emission signal of LMD manufacture of specimen 1, unfiltered (left) and filtered (right) with corresponding frequency spectrograms

To specify defect noise events with distinct frequencies, particular audio periods were selected manually where clear audio anomaly events occur. Performing frequency spectrographs for these audio periods, distinct frequency peaks could be identified between 11000 and 18000 Hz, especially with peaks at 11500 Hz, 12900 Hz and 16000 Hz. Thus, for further audio emission analysis, all frequencies outside of the bandwidth 11000 to 18000 Hz are weakened and filtered using a negative audio gain of -12 dB.

By cutting frequencies below 2000 Hz and weakening frequencies  $< 11000$  Hz and  $> 18000$  Hz, lower data streams result for further audio emission analysis. The diagrams on the right side in Fig 2. show the audio signal of specimen 1 after applying frequency filters. The periodic peaks with an amplitude up to  $\pm 0,095$  indicate each welding seam of the NiTi structure and are considered as regular audio process emissions. Audio signals with an amplitude between  $\pm 0,095$  and  $\pm 0,125$  occur irregularly and will be allocated to light defect audio signals. Appearing audio signals with a normalized amplitude  $> 0,125$  occur strongly irregularly and are considered as heavy defect audio signals. To quantify the considered defect audio signals, normalized amplitude thresholds are defined to  $\pm 0,095$  and  $\pm 0,125$ . By applying these thresholds to all audio signal files, the following acoustic emission monitoring values are defined:

- counts of light defect audio signals,  $n_{ad,l}$
- counts of heavy defect audio signals,  $n_{ad,h}$
- time to first heavy defect audio signal,  $t_{ad,h}$

The application of both thresholds and the automated generation of  $n_{ad,l}$ ,  $n_{ad,h}$ ,  $t_{ad,h}$  were performed by using *MATLAB*. The corresponding diagram for specimen 1 is depicted in Fig. 3, where values above threshold 1 ( $> 0,095$ ) are illustrated in blue and values above threshold 2 ( $> 0,125$ ) are illustrated in red.

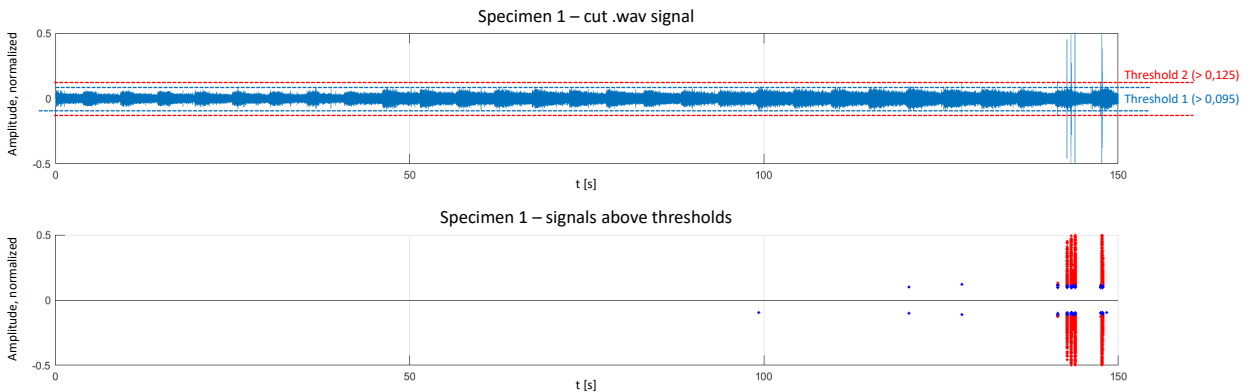


Fig. 3. Filtered acoustic emission signal with illustration of threshold 1 and threshold 2 (top) and resulting acoustic emission signal above threshold 1 and 2 (bottom)

The diagram shows, that overall a low amount of defect audio signals occur. Especially the last two welding seams in layer 3 produce audio emissions, that can be considered as defect audio emissions. Heavy defect audio signals occur only within the last two welding seams and show high amplitude peaks between  $t = 140$  s and  $t = 150$  s. The counts of light defect audio signals ( $n_{ad,l}$ ), the counts of heavy defect audio signals ( $n_{ad,h}$ ) and the time to first heavy defect audio signal ( $t_{ad,h}$ ) are summarized in Table 2 for each specimen.

Table 2. Acoustic emission monitoring values  $n_{ad,l}$ ,  $n_{ad,h}$  and  $t_{ad,h}$  of specimen 1 – 7

# of specimen	unit	1	2	3	4	5	6	7
$n_{ad,l}$	[-]	3911	1331	4434	1496	4556	3915	5724
$n_{ad,h}$	[-]	2995	933	2915	1303	3154	2557	3409
$t_{ad,h}$	[s]	141,45	137,53	116,56	152,22	122,13	121,27	97,64

To evaluate the quality of the defined audio emission monitoring values, the correlation between monitoring values and degree of delamination have to be investigated. The evaluation is summarized in chapter 3.3 after the identification of the degree of delamination in chapter 3.2.

### 3.2. Identification of degree of delamination

The as-built NiTi specimen are shown in Fig. 4. The side view of the specimen shows the x-z plane of the specimen, where the z-direction is the positive layer build up direction. Thus, the shown x-z plane indicates the front and beginning of the NiTi structures.

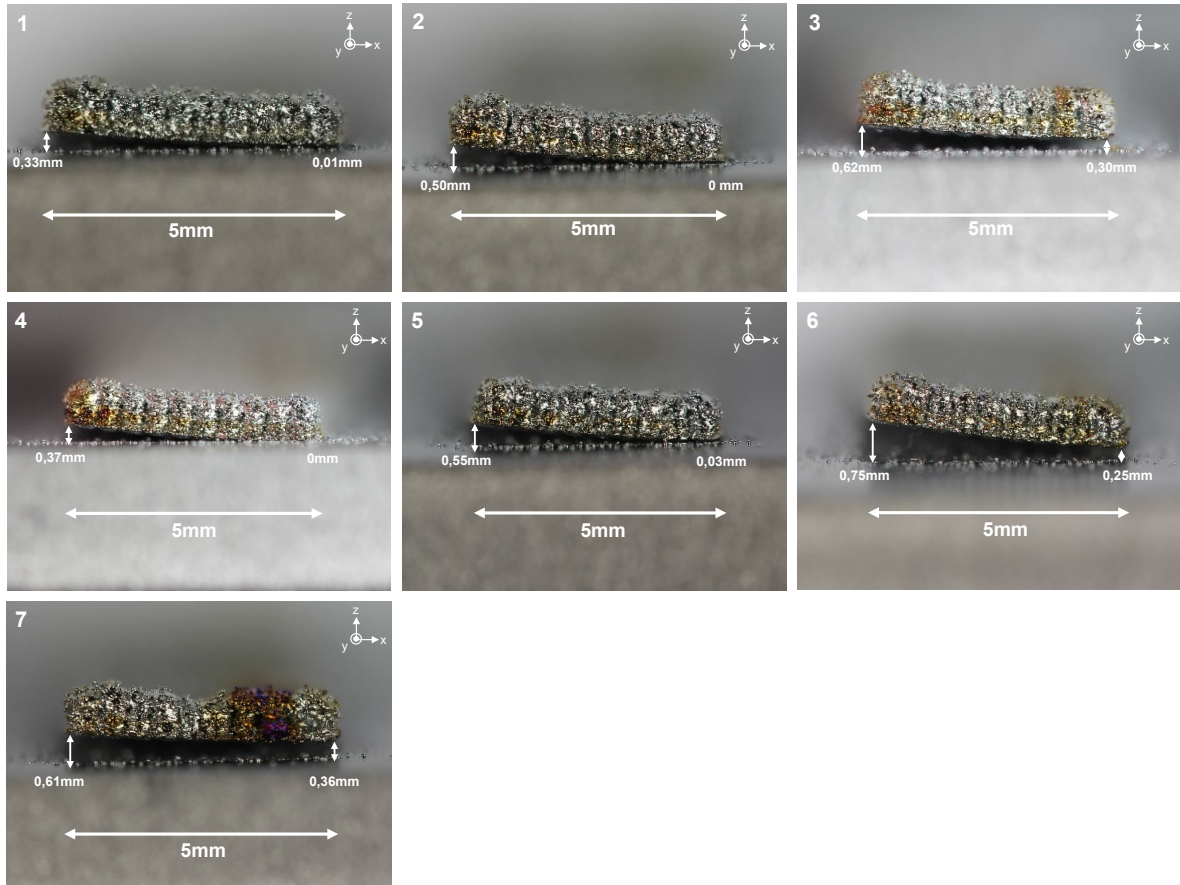


Fig. 4. Front view (x-z plane) of LMD processed NiTi structures of specimen 1 – 7

As expected, every LMD structure delaminated while processing. Specimen 1, 2 and 5 show none to minor oxidation signatures. Specimen 3, 4 and 6 show medium oxidation signatures, while specimen 7 is characterized by strong oxidation signatures. To identify the degree of delamination, the average gap between substrate material and deposited NiTi structure is calculated. The average gap size is defined as  $z_{gap}$ . Input values for the calculation of  $z_{gap}$  are  $z_{gap}(x=0\text{mm})$  and  $z_{gap}(x=5\text{mm})$ . The results for the average gap size are summarized in Table 3 below.

Specimen 7 was manufactured with a process parameter manipulation to trigger further defect formation. In each layer, 3 centered welding seams were performed with a change of laser spot diameter from 0,48 mm to 3,52 mm. Specimen 4 was performed without process parameter manipulation under the same  $O_2$  level concentration. The process parameter manipulation in specimen 7 lead to comparatively strong delamination and oxidation signatures. Especially the center of the of the deposited structure is characterized by smaller resulting layer height and strong oxidation signatures.

Table 3. Measurement values for the evaluation of the degree of delamination for specimen 1 – 7

# of specimen	unit	1	2	3	4	5	6	7
$z_{gap}(x=0\text{mm})$	[mm]	0,32	0,50	0,62	0,37	0,55	0,75	0,61
$z_{gap}(x=5\text{mm})$	[mm]	0,01	0,01	0,29	0,00	0,03	0,25	0,36
$z_{gap}$	[mm]	0,17	0,25	0,46	0,19	0,29	0,50	0,49

The calculated values show, that the highest degree of delamination occurred in specimen 6 and specimen 7. These values confirm the assumption that deviating DED process parameters and higher residual  $O_2$  concentrations result in higher degree of delamination. The correlation of the degree of deformation and its acoustic emissions is analyzed in chapter 3.3 – the correlation to residual  $O_2$  concentration is investigated in chapter 3.4.

### 3.3. Correlation of acoustic emission monitoring values and degree of delamination

To evaluate the correlation of the defined acoustic emission monitoring values,  $z_{gap}$  is plotted over  $t_{ad,h}$ ,  $n_{ad,l}$  and  $n_{ad,h}$  in Fig. 5. Additionally each diagram contains a linear trend line. Exponential, potential or logarithmic trend lines show larger deviations to its corresponding data points, thus the investigation of correlation is focused on linear dependencies.

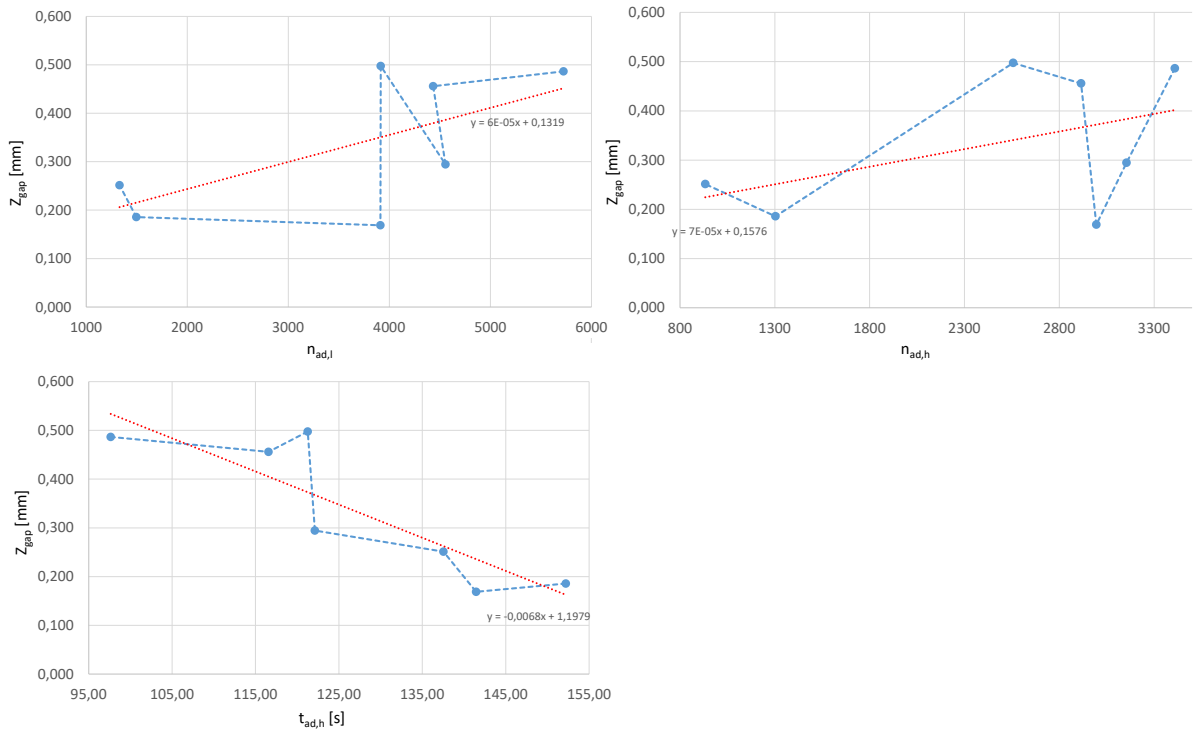


Fig. 5. Plots of degree of delamination  $z_{gap}$  over acoustic emission monitoring values  $n_{ad,l}$ ,  $n_{ad,h}$  and  $t_{ad,h}$

The measurement value  $t_{ad,h}$  correlates negative linear to  $z_{gap}$ , while  $n_{ad,h}$  and  $n_{ad,l}$  show a positive linear correlation to  $z_{gap}$ . All plots point out at least one data point that has a high offset to the linear trend line. To identify the most suitable acoustic emission monitoring value, the correlation coefficient is calculated for each data set, based on its mean values, standard values and covariance. The values are summarized in Table 4 below.

Table 4. Statistical key values for the evaluation of correlation coefficients of acoustic emission monitoring values and degree of delamination

	unit	X: $t_{ad,h}$	X: $n_{ad,l}$	X: $n_{ad,h}$	Y: $z_{gap}$
Mean value	[mm], [s]	126,97 s	3623,23	2466,57	0,334 mm
Standard deviation	[mm], [s]	16,83 s	1506,56	890,83	0,132 mm
Covariance	[mm], [s]	-1,93 s	126,76	56,85	-
Correlation coefficient	-	-0,87	0,64	0,48	-

The evaluation shows, that  $t_{ad,h}$  correlates highly negative (-0,87) to the degree of deformation  $z_{gap}$ . Consequently, monitoring of  $t_{ad,h}$  is recommended when monitoring of structural delamination is required.



When LMD process parameters change within the manufacture of LMD structures, defects can occur instantly. Parameter set 4 and parameter set 7 simulate this event, by changing the laser spot diameter from 0,48 mm to 3,52 mm for 3 welding seams each layer. Resulting defects can be identified optically in Fig. 4. Additionally, the measurement data of  $t_{ad,h}$  also indicates early heavy defect audio signals after 97,6 s, respectively 1,5x earlier than compared to parameter set 4. Therefore, defect formation can be observed with an acoustic monitoring system and data evaluation focused on the detection of time that passes, until heavy defect audio emissions occur ( $t_{ad,h}$ ).

To enable In-Process detection of defect audio signals respectively defect formation, a live data evaluation unit has to be set up. The data evaluation unit has to be connected directly to the audio interface and offer visual output systems for machine users. Live cutting and filtering of audio signals dependent on individual amplitude thresholds and instant output have to be performed by the data evaluation system. Additionally, input systems and commands should be possible to adjust individual frequency filter mechanisms and edit amplitude thresholds. Data evaluations system, such as single board computers and python based live scripts to enable data input, filter-, detection- and output-functions have been tested and are considered as suitable data evaluation system.

### 3.4. Correlation of acoustic emission values to residual $O_2$ concentration

To evaluate the influence of different  $O_2$  concentrations within the LMD process chamber on the formation of delamination, the residual  $O_2$  concentration was measured and controlled during the LMD manufacture of NiTi structures. The degree of deformation  $z_{gap}$  and the time to the first heavy defect audio signal,  $t_{ad,h}$  is plotted over the residual  $O_2$  concentration in ppm in Fig. 6. Since parameter set 7 was modified to trigger defects, only parameter set 1 – 6 are analyzed.

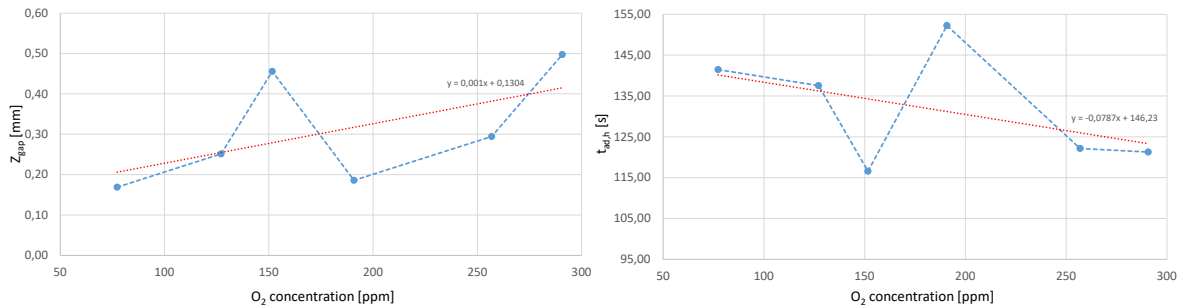


Fig. 6. Plots of degree of delamination  $z_{gap}$  (left) and  $t_{ad,h}$  (right) over  $O_2$  concentration

As expected, it is identifiable that higher  $O_2$  concentrations result in higher degree of deformation, which is supported by a positive linear correlation of  $z_{gap}$  to  $O_2$  concentration. Nevertheless, the correlation coefficient calculates to 0,57 which indicates a lower positive linear correlation of  $z_{gap}$  to  $O_2$  concentration. This comparatively low correlation coefficient results due to one major offset, where a higher degree of deformation with  $z_{gap} = 0,46$  occurred at 152 ppm  $O_2$  concentration.

Similar behavior is recognizable when analyzing the correlation of  $t_{ad,h}$  to  $O_2$  concentration. Two major offset are identifiable at 152 ppm and at 190 ppm  $O_2$  concentrations, where heavy defect audio signals were detected after 116,56 s and 152,22 s. This results in a lower correlation coefficient of -0,45 describing a negative linear correlation of  $t_{ad,h}$  to  $O_2$  concentration.

Therefore, the achieved measurement data shows, that similar delamination behavior can occur at O<sub>2</sub> concentrations of 80 ppm and 200 ppm. The relatively low amount of O<sub>2</sub> concentration data offers no reliable dependencies between  $z_{gap}$ , O<sub>2</sub> concentration. And  $t_{ad,h}$ , O<sub>2</sub> concentration. Thus, multiple oxygen sensor setups are recommended for further investigations.

#### 4. Conclusion

Acoustic emissions and O<sub>2</sub> concentration were monitored and captured during the LMD manufacture of NiTi structures. Defects such as structural delamination were triggered by the pre-selection of LMD process parameters. After manual filtering of acoustic frequencies and amplitudes, three acoustic monitoring measurement values were defined: (1) counts of light defect audio signals, (2) counts of heavy defect audio signals and (3) time to first heavy defect audio signal. Further, the degree of delamination has been identified for each specimen.

It is shown, that the acoustic monitoring measurement value time to first heavy defect audio signal  $t_{ad,h}$  highly correlates with the degree of delamination. Triggered defects by LMD parameter manipulation resulted in strong defect signatures and could be identified by acoustic emission monitoring. A defect monitoring concept has been derived by  $t_{ad,h}$ , to enable an In-Process control concept.

The influence of different O<sub>2</sub> levels within the process chamber on the structural delamination process have been investigated. A low correlation of O<sub>2</sub> concentration on the resulting degree of delamination has been identified, multiple oxygen sensor setups are recommended for further investigations.

#### References

- Engblom E., 2018. Effect of oxygen concentration in build chamber during laser metal deposition of Ti-64 wire. Digitala Vetenskapliga Arkivet, DiVA-portal.
- Gaia, H., Liou, F., 2016. Defects monitoring of laser metal deposition using acoustic emission sensor. *International Journal of Advanced Manufacturing Technology* 90, p. 561 – 574.
- Halani, P. R., Kaya, I., Shin, Y.C., Karaca, H., E., 2012. Phase transformation characteristics and mechanical characterization of nitinol synthesized by laser direct deposition. *Materials Science & Engineering A* 559, p. 836 – 843.
- Kaufmann, G. B., Mayo, I., 1997. The story of nitinol: The serendipitous discovery of the memory metal and its applications. *The Chemical Educator* 2, 1-21.
- Krishna, B. V., Bos, S., Bandyopadhyay, A., 2007. Laser processing of net-shape NiTi shape memory alloy. *Metallic Material Transition A* 38, p. 1096-1103.
- Scheitler, C., Hentschel, O., Krebs, T., Nagulin, K. Y., 2017. Laser metal deposition of NiTi shape memory alloy on Ti sheet metal: Influence of preheating on dissimilar build-up. *Journal of Laser Applications* 29, Issue 2.
- Taheri, H., Koester, L. W., Bigelow, T., A., Faierson, E. J., Bond, L. J., 2019. In Situ Additive Manufacturing Process Monitoring With an Acoustic Technique: Clustering Performance Evaluation using K-Means Algorithm. *Journal of Manufacturing Science and Engineering* 141.
- Tang, Z., Liu, W., Wang, Y., Saleheen, K. M., Liu, Z., Peng, S., Zhang, Z., Zhang, H., 2020. A review on in situ monitoring technology for directed energy deposition of metals. *The International Journal of Advanced Manufacturing Technology* 108, p. 3437 – 3463.
- Wang, F., Mao, H., Zhang, D., Zhao, X., Shen, Y., 2008. Online study of cracks during laser cladding process based on acoustic emission technique and finite element analysis. *Applied Surface Science*, Volume 255, Issue 5, Part 2, p. 3267 – 3275.